Future Energy
Open Access Journal
ISSN 2832-0328

August 2026| Volume 05 | Issue 03 | Pages 50-58

Journal homepage: https://fupubco.com/fuen

https://doi.org/10.55670/fpll.fuen.5.3.4

Future Publishing LLC

Article

Integrated energy, exergy, and techno-economic analysis of an off-grid hybrid solar-battery-generator system for disaster-relief container homes in Ankara, Türkiye

Kadir Aydın*
Department of Mechanical Engineering, OSTİM Technical University, 06374 Ankara, Türkiye

ARTICLE INFO

Article history:
Received 26 February 2026
Received in revised form
04 June 2026
Accepted 06 July 2026

Keywords:
Off-grid hybrid energy, Exergy analysis,
Glass–glass photovoltaics, $LiFePO_4$ storage,
Double-wall solar boiler,
Techno-economic analysis

*Corresponding author
Email address:
kadir.aydin@ostimteknik.edu.tr

DOI: 10.55670/fpll.fuen.5.3.4

ABSTRACT

The 6 February 2023 Kahramanmaraş earthquakes (Mw 7.7 and Mw 7.6) left more than three million people homeless in Türkiye and, as of February 2025, over 649,000 people still reside in container settlements, for which reliable grid-independent energy provision remains an unsolved challenge. This paper presents the integrated design, first- and second law (energy and exergy) thermodynamic analysis, annual simulation, and techno-economic and environmental assessment of a mobile hybrid energy production, storage, and management system built for a 21 m^2 disaster-relief container home in Ankara (39.93°N), using commercially procured equipment. The system couples a 3.57 kWp array of six 595W glass–glass modules, with a planned roll-bond photovoltaic–thermal retrofit, a 5.12 kWh $LiFePO_4$ battery, an 8.2 kW dual-MPPT inverter, a 7.5 kVA dual-fuel generator with exhaust heat recovery, a 3.42 m^2 aluminium flat-plate solar-thermal field charging a 185 L (net) double-wall chromium boiler for domestic hot water and supplementary heating, and a single 12,000 BTU A++ inverter air conditioner dedicated to cooling (heat-pump heating retained only as emergency backup), all under a PLC-based EMS/SCADA. A 35° sawtooth mounting structure is designed, and its tilt optimization and inter-row shading are analyzed under the constraint of a 3 m roof depth. The annual electricity yield is 4,430 kWh (parallel-mounted), rising to 4,960 kWh at the 35° optimum, against ~1,740 kWh electrical demand, giving full summer autonomy and 60–85 h of winter generator run-time. The combined first-law efficiency reaches 68% in cogeneration mode; the overall second-law efficiency is ~24% (sustainability index 1.32), the low-temperature collector and the indirect double-wall boiler being the principal exergy-destruction sites. Against a continuous generator baseline, the system pays back in ~6 years and avoids ~2,770 kg CO_2/yr (~69 t over 25 years).

1. Introduction

Türkiye lies across one of the world's most seismically active regions, and the 6 February 2023 Kahramanmaraş earthquakes, recorded by the Disaster and Emergency Management Authority (AFAD) as Mw 7.7 (Pazarcık) and Mw 7.6 (Elbistan), constitute the deadliest natural disaster in the country's modern history, with 53,537 fatalities, roughly 280,000 buildings destroyed or severely damaged, and some 3.3 million people displaced [1,2]. The housing and disaster authorities deployed tens of thousands of standardized 21 m^2 container dwellings; as of February 2025, 649,632 people still lived in 395 container cities [2]. Although these containers provide rapid, structurally sound shelter, their energy supply remains precarious: post-disaster grids are frequently down for weeks, portable generators incur high fuel cost and emissions, and gas heating depends on a fragile supply chain. Ankara, however, receives roughly 1,500-1,600 kWh/m^2 of annual global horizontal irradiation with 4.1-4.4 peak-sun-hours per day [3], an under-exploited resource for emergency settlements. Hybridizing photovoltaic electricity with solar-thermal heat, battery storage, and a fuel-based backup has been well studied for stand-alone use [4-7], and photovoltaic-thermal (PVT) collectors enhance the combined exploitation of the solar resource [8]. Exergy (second law) analysis, grounded in the Petela relation for the exergy of solar radiation [9], complements energy balances by revealing

where the thermodynamic quality of the resource is destroyed [10,11]. Glass–glass (bifacial-capable) PV modules offer an additional advantage: a symmetric laminate lowers the operating temperature coefficient and improves long-term degradation behavior relative to glass–backsheet modules [12]. $LiFePO_4$ batteries dominate stationary off-grid storage for their thermal stability and long life (round-trip efficiency of 92-98% and 3,000-6,000+ cycles) [13-16], a decisive safety advantage in fire-prone settings.

Nevertheless, prior off-grid sizing studies, typically using HOMER Pro [6,7], focus on the electrical subsystem and rarely integrate the thermal loads that dominate dwelling demand in a continental climate, whereas container-housing studies address envelopes and structure [17-21] rather than a fully coupled multi-source energy system. To the author's knowledge, no previous work reports an integrated energy–exergy–economic analysis of such a system, built from commercially procured components, for seismically driven emergency housing in a cold-semi-arid climate. The present study addresses this gap and contributes:
(i) a coupled thermal-load and annual energy-balance model; (ii) a component-resolved first- and second-law analysis including the indirect double-wall boiler; (iii) a 35° mounting design with tilt-optimization and inter-row-shading analysis for a constrained roof; (iv) a techno-economic and sensitivity assessment benchmarked against a continuous-generator baseline; and (v) an environmental assessment of avoided CO_2. A distinctive, thermodynamically justified feature is the division of duties, whereby the inverter air conditioner provides cooling, while renewable solar-thermal energy provides primary heating and hot water, with the heat pump reserved for emergency heating only.

2. System description and methodology

2.1 System configuration and procured equipment

The mobile hybrid energy production, storage, and management system (Figure 1) integrates six subsystems under a PLC-based EMS/SCADA layer; the container itself was supplied by AFAD. Electrical generation uses six 595W glass–glass modules (3.57 kWp) in a 3-series×2-parallel arrangement feeding the dual-MPPT inputs of an 8.2 kW off-grid inverter; an aluminum roll-bond PVT retrofit is a planned enhancement [4]. Storage is a 5.12 kWh (51.2 V, 100 Ah) $LiFePO_4$ pack, and backup is a 7.5 kVA dual-fuel inverter generator with exhaust heat recovery. Domestic hot water (DHW) and supplementary heating are provided by a 3.42 m^2 (two 0.90×1.90 m) aluminum flat-plate collector field charging a 185 L net horizontal double-wall chromium boiler, in which the collector glycol circulates in the outer jacket and indirectly heats potable water in the inner 304-stainless tank; an optional electric resistance element and a generator-exhaust heat exchanger supplement it, and fan-coils distribute heat. Cooling is provided by a single 12,000 BTU A++ R32 inverter air conditioner; its heat-pump heating mode is reserved for emergency use during extreme cold.

2.2 Building thermal-load model

The container (7.0×3.0×2.65 m; 21 m^2; 43.7 m^3) was modeled by the TS 825 degree-day method and ASHRAE load procedures [20,21], with envelope transmittances U_{wall} = 0.465, U_{roof} = 0.407, U_{floor} = 0.791, U_{window} = 2.9 and U_{door} = 2.2 W/m^2 K and an infiltration rate of 0.8 1/h (air changes per hour) [19]. The transmission-plus-infiltration heat-loss rate is given by Eq (1):

$$Q_{loss} = (\Sigma\, U_i A_i + 0.34\, n\, V)\, \Delta T \quad (1)$$

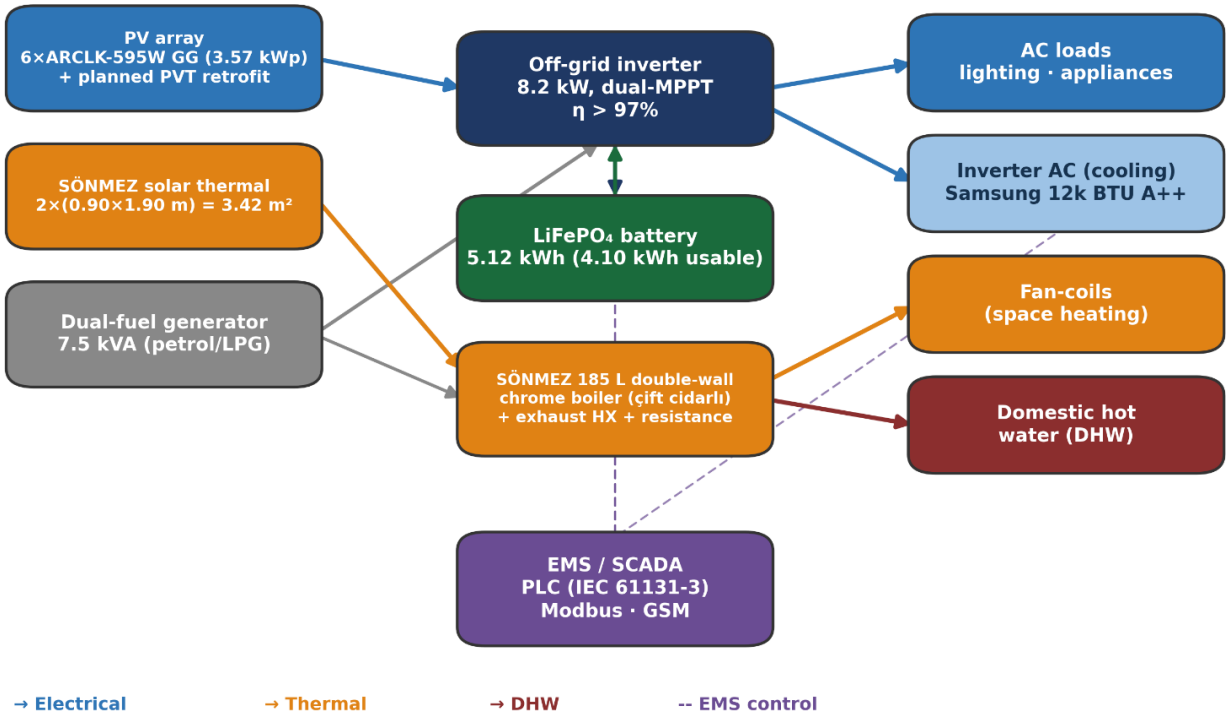

Figure 1. Architecture and energy-flow topology of the mobile hybrid energy production, storage, and management system

2.3 Energy modeling

The monthly PV yield follows Eq. (2), with a performance ratio PR (0.76–0.83) accounting for temperature, soiling, wiring, MPPT, and inverter losses; the flat-plate collector output follows the steady-state relation of Eq. (3), with optical efficiency $\eta_0 \approx 0.78$ and loss coefficient $a_1 \approx 3.75$ W/m^2 K:

$$E_{PV} = P_{STC} \cdot PSH \cdot PR \quad (2)$$

$$Q_{th} = A_c\,[\eta_0\,G - a_1\,(T_m - T_a)] \quad (3)$$

2.4 Exergy modeling

Taking the dead state at T_0 = 285 K (the Ankara annual mean), the specific exergy of solar radiation is given by the Petela relation, Eq. (4), with the sun as a T_s = 5778 K radiation source:

$$\psi_{sol} = 1 - \frac{4}{3}\frac{T_0}{T_s} + \frac{1}{3}\left(\frac{T_0}{T_s}\right)^4 \quad (4)$$

The indirect double-wall boiler is characterized by a jacket charging effectiveness ε, Eq. (5), which quantifies the additional irreversibility introduced by heating the potable inner tank through the glycol jacket rather than a direct serpentine:

$$\varepsilon = \frac{T_{tank,out} - T_{tank,in}}{T_{jacket,in} - T_{tank,in}} \quad (5)$$

The air conditioner's second-law efficiencies in heating and cooling are referenced to their Carnot limits, Eq. (6), and the sustainability index follows from the overall exergy efficiency, Eq. (7):

$$\psi_{HP} = \frac{COP}{COP_{Carnot}} \quad , \quad \psi_{AC} = \frac{EER}{EER_{Carnot}} \quad (6)$$

$$SI = \frac{1}{1-\psi} \quad (7)$$

2.5 Techno-economic and environmental modeling

The levelized cost of energy and the capital recovery factor are given by Eq. (8), with a discount rate of i = 10% over n = 25 years; avoided emissions use a Turkish grid factor of 0.45 kg CO_2/kWh (IEA range 0.4–0.5) [3] and a fuel factor for displaced LPG. The R32 refrigerant has GWP_{100} = 675 and zero ozone-depletion potential (ASHRAE A2L).

$$LCOE = \frac{C_0 \cdot CRF + C_{O\&M}}{E_{useful}} \quad , \quad CRF = \frac{i\,(1+i)^n}{(1+i)^n - 1} \quad (8)$$

3. Results and discussion

3.1 Solar resource, tilt optimization, and energy yield

Figure 2 shows the monthly solar resource and the PV and solar-thermal yields. The 4.25 mean peak-sun-hours give an annual PV generation of 4,430 kWh in the as-built parallel-to-roof configuration, rising to 4,960 kWh at the 35° optimum (Fig. 3a), while the 3.42 m^2 collector field delivers ~1,870 kWh of useful heat. Figure 3a confirms that for Ankara, the annual yield is maximized near 33° and that 35° lies within 1% of the optimum, justifying the design tilt; the as-built parallel mount sacrifices ~11%. The 35° mounting is realized as a sawtooth frame (collectors low at the south edge, two PV rows behind). Figure 3b quantifies the geometric tension on the 3 m-deep roof: a fully shadow-free winter pitch requires ≈2.23 m, whereas only ~1.0-1.1 m is available, so some winter inter-row shading is unavoidable. This is mitigated by placing the collectors in the low front row and by splitting the array 3+3 across two MPPT inputs so that partial shading of one row does not drag down the other.

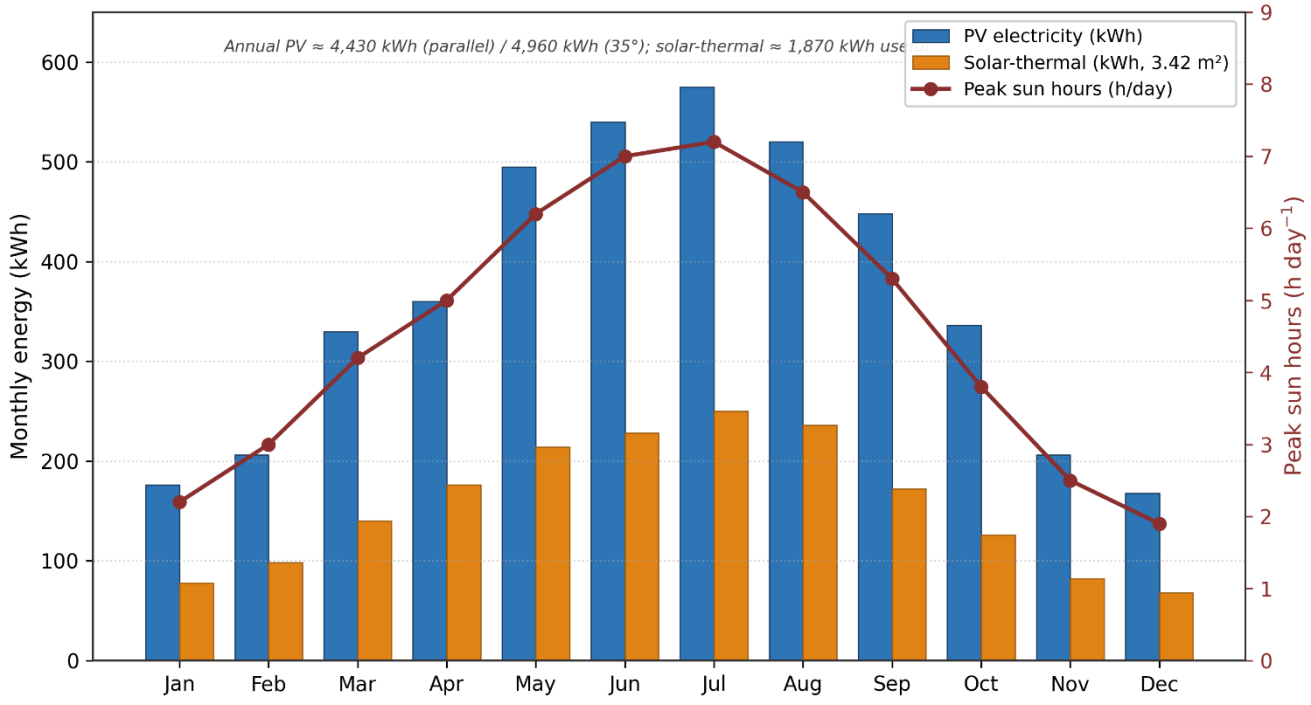

Figure 2. Monthly solar resource and PV and solar-thermal (3.42 m^2) energy yields for Ankara

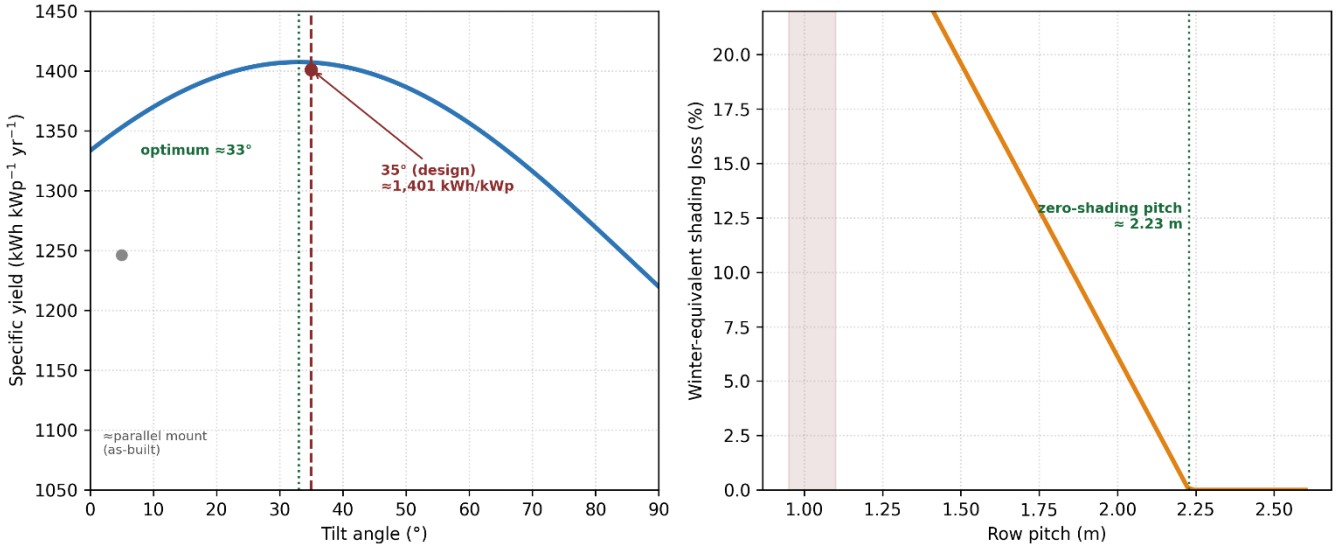

(a) (b)

Figure 3. (a) Annual PV specific yield vs. tilt for Ankara, (b) inter-row shading loss vs. row pitch at 35°

3.2 Annual energy balance and autonomy

Figure 4 contrasts the daily PV supply with demand and the resulting generator dispatch. From April to October, the array exceeds demand, and the system is fully autonomous, the battery covering the 22:00-07:00 night load (1.6-3.0 kWh against 4.10 kWh usable). In December-February, low irradiation reduces PV output to 5.6-6.5 kWh/day against a demand of 11-14 kWh/day, requiring 1.0-1.5 h/day of generator operation (60-85 h/yr). With ~1,740 kWh of demand against 4,430 kWh generated, annual electrical self-sufficiency ranges from 79% to 95%. The thermal side is more constrained. The 3.42 m^2 collector field supplies ~1,870 kWh, covering roughly 55% of the 3,494 kWh DHW demand; the 185 L boiler, being primarily a DHW vessel, offers limited thermal storage for space heating. Consequently, sustained winter space heating depends on the generator-exhaust contribution (~550 kWh) and, in extreme cold, on the emergency heat-pump mode, while the planned PVT retrofit (~3,400 kWh) would substantially raise the solar fraction. Because both the solar-thermal and PV supplies are lowest exactly when heating demand peaks, winter heating is the binding design constraint and the principal justification for retaining the generator and the emergency heat-pump fallback.

3.3 First and second law performance

Figure 5 compares component energy and exergy efficiencies. The glass–glass modules convert 21.0% of incident energy to electricity, but electricity being pure exergy, their exergy efficiency is higher at 24.7%; their symmetric laminate also lowers the temperature coefficient, marginally improving hot-month output [12]. The flat-plate collector shows the opposite pattern, 50% energy but only 7.7% exergy efficiency, because high-quality solar radiation is degraded to ≤60 °C heat. The indirect double-wall boiler introduces a second exergy penalty: the jacket imposes an additional temperature drop between the glycol and potable water, reducing the effective charging exergy efficiency relative to a direct serpentine. The battery (93%) and inverter (97%) are near-ideal, and the air conditioner attains 8.7% exergy efficiency in cooling and 21.5% in its backup heating mode. Figure 6 traces the exergy cascade: PV conversion destroys 36 percentage points of the incident solar exergy, and the thermal collector a further 34, so only ~24% emerges as a useful product, giving an overall second-law efficiency of ~24% and a sustainability index of 1.32, consistent with roll-bond and nanofluid PVT systems [4,8,10]. The low-temperature collector and the indirect boiler are the dominant loss sites, indicating that evacuated-tube collectors or full PVT operation would yield the greatest second-law improvement.

3.4 Climate-control subsystem

Figure 7 examines the air conditioner. A single 12,000 BTU unit (3.51 kW cooling, 3.81 kW heating; SEER 6.1, SCOP 3.9) covers the 1.76 kW peak cooling load with a 99% margin and the 2.33 kW peak heating load with an 81% margin (Figure 7a). Procuring one inverter unit for cooling, rather than the originally specified two indoor-unit multi-split, saved ≈ 40,800 TL, as a multi-split-plus-installation quotation reached ~69,700 TL, and is thermodynamically sound for this small, low-humidity, open-plan space. Heating is nonetheless assigned to the renewable solar-thermal circuit: although the heat pump's SCOP of 3.9 far exceeds resistance heating (Figure 7b), its COP derates sharply below 0 °C, so using it as the primary winter heater would burden the already-scarce winter electricity supply; reserving it for emergencies protects night-time battery autonomy while retaining a high-efficiency fallback.

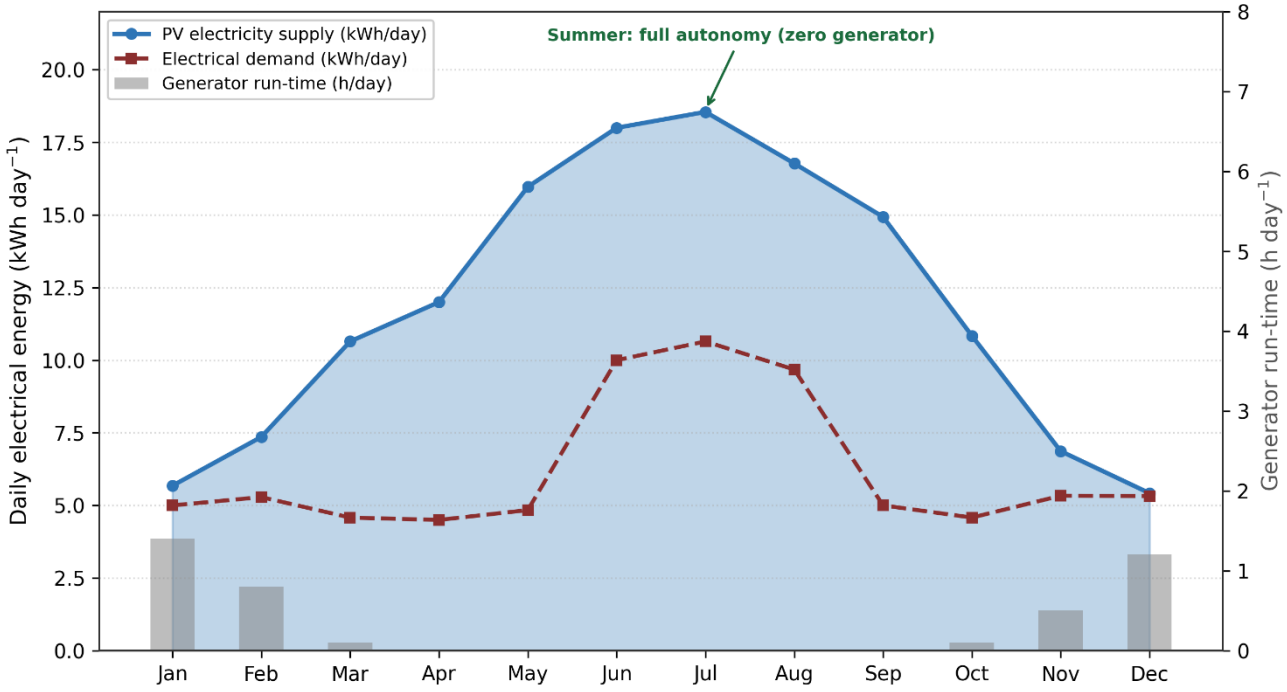

Figure 4. Monthly electrical energy balance (PV supply vs. demand) and generator run-time

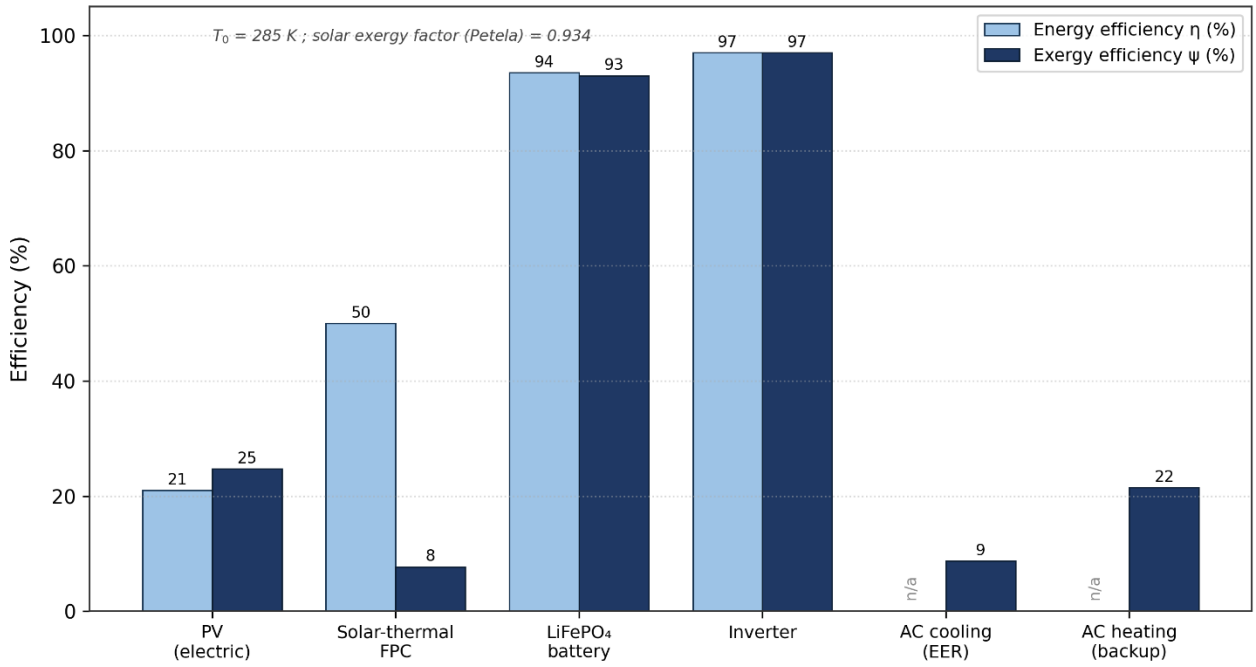

Figure 5. Component-level first law (energy) and second law (exergy) efficiencies. T_0 = 285 K.

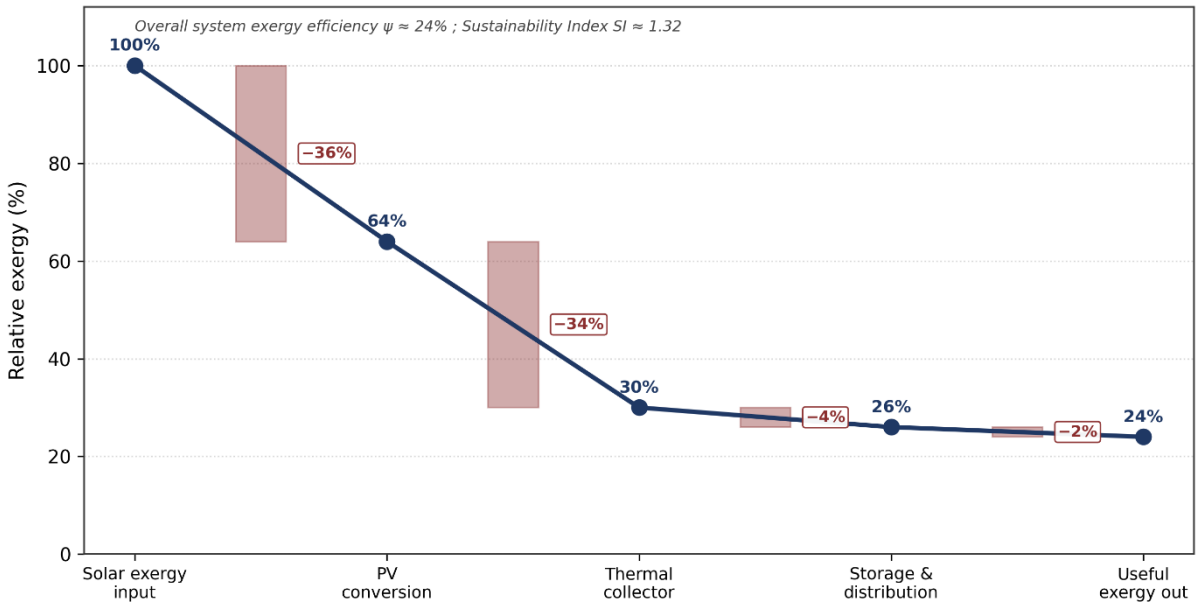

Figure 6. Exergy cascade and stage-wise destruction across the mobile hybrid energy production, storage, and management system conversion chain

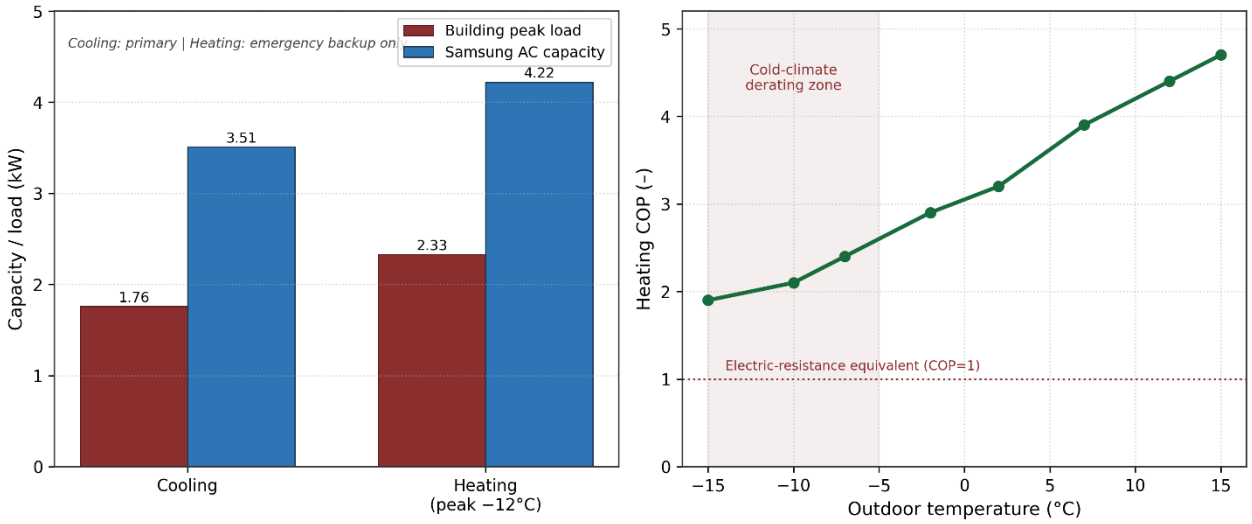

(a) (b)

Figure 7. (a) Air-conditioner capacity vs. building peak loads; (b) heat-pump COP derating with ambient temperature

3.5 Techno-economic assessment and sensitivity

The prototype capital cost is ≈ 438,000 TL (Figure 8a), the container contributing nothing. Against the grid retail tariff (~2.6 TL/kWh) the off-grid system is not cost-competitive, its system LCOE of ~6.2 TL/kWh reflects the intrinsic battery-and-generator premium [6,7], but against the disaster-zone reality of a continuous generator plus LPG it saves ≈ 75,000 TL/yr and reaches parity in ~6 years (Figure 8b), with a positive 25-year net present value. A one-at-a-time sensitivity analysis shows the LCOE is most sensitive to battery capital cost (elasticity ≈ −0.5) and to collector area and solar irradiation (≈ +0.1 to +0.2 each), and least sensitive to discount rate over 8–12%; a projected 30% fall in $LiFePO_4$ price would cut the LCOE by ~15% and shorten payback by ~1.8 years.

The economic case is therefore driven by energy autonomy and independence in fuel logistics rather than by tariff arbitrage.

3.6 Environmental assessment

Figure 9 quantifies avoided emissions: 1,994 kg CO_2/yr from displaced grid electricity, 625 kg from displaced LPG heating, and 150 kg from exhaust recovery, totaling ≈ 2,770 kg CO_2/yr and ≈ 69 t over 25 years per unit. Scaled across the hundreds of thousands of container dwellings still in service, the aggregate mitigation is substantial, while the R32 refrigerant (GWP_{100} = 675) limits the direct climate impact of the cooling subsystem relative to legacy refrigerants.

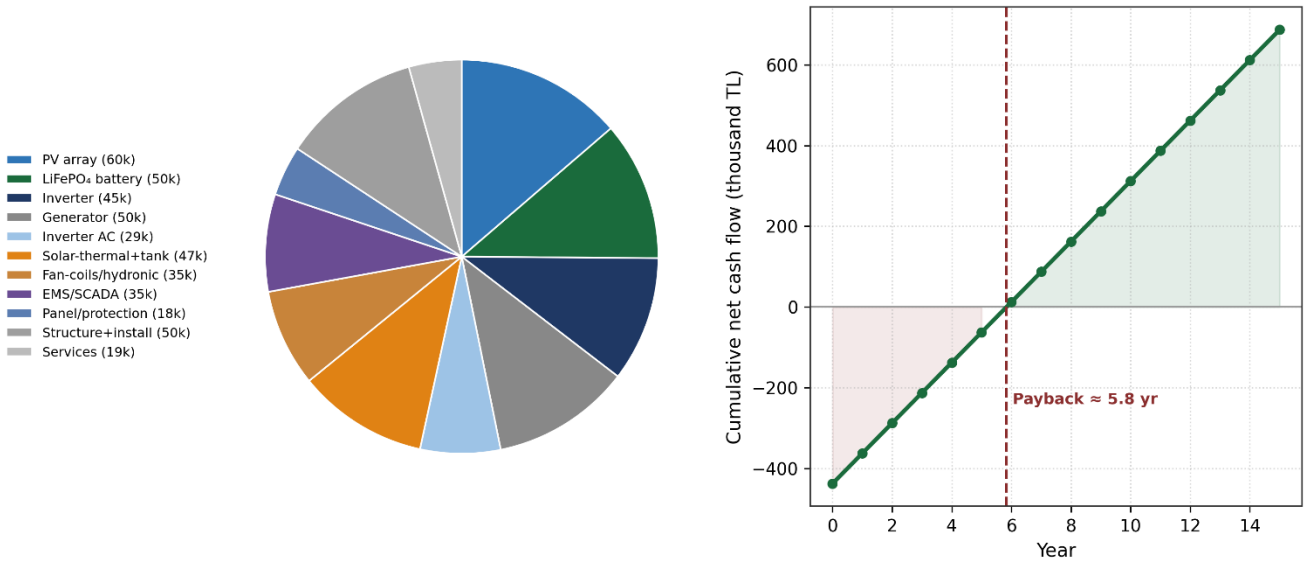

Figure 8. (a) Capital-cost breakdown, (b) cumulative cash flow against a continuous-generator baseline

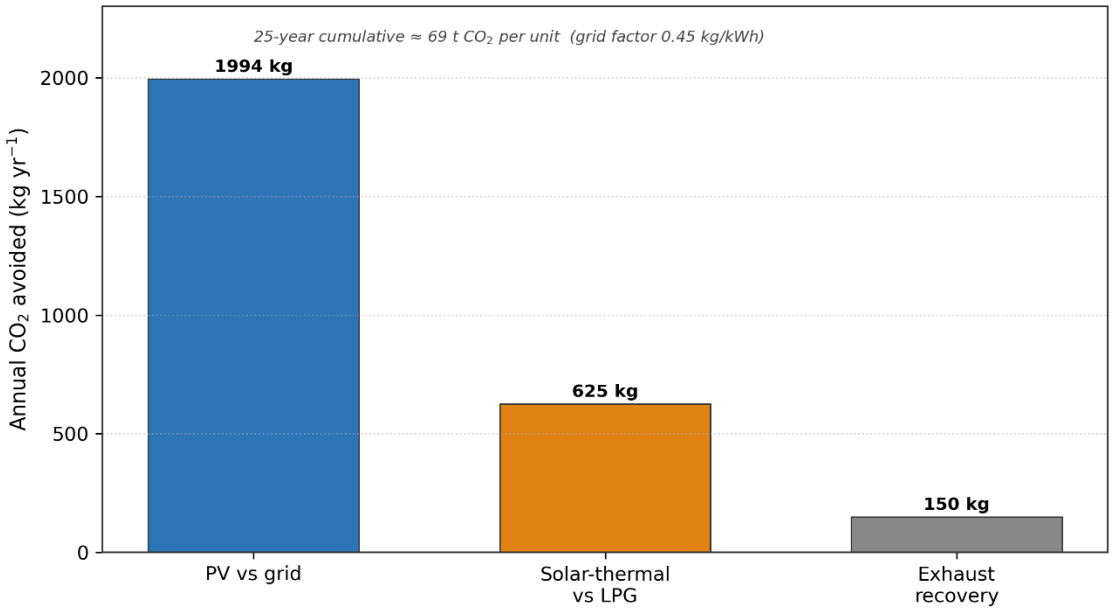

Figure 9. Annual avoided CO_2 emissions by source (grid factor 0.45 kg CO_2/kWh)

4. Conclusions

An off-grid hybrid solar–battery–generator system, built from commercially procured equipment, was designed and analyzed for a 21 m^2 disaster-relief container home in Ankara, integrating first- and second-law thermodynamics, annual simulation, a 35° mounting design, and techno-economic and environmental assessments. The principal findings are:

- The 3.57 kWp glass-glass array generates 4,430 kWh/yr (parallel), rising to 4,960 kWh at 35°, against ~1,740 kWh demand, giving full summer autonomy and only 60-85 h/yr of winter generator operation.
- For Ankara, the annual yield peaks near 33° and 35° is within 1% of optimum; however, the 3 m roof depth precludes a shadow-free 35° row pitch (≈2.23 m needed vs ~1.0-1.1 m available), so collectors are placed low at the front and the array is split 3+3 across two MPPTs to limit shading losses.
- The combined first-law efficiency reaches 68% in cogeneration mode; the overall exergy efficiency is ~24% (SI = 1.32), the low-temperature collector and the indirect double-wall boiler being the dominant exergy-destruction sites.
- Assigning cooling to a single A++ inverter unit and heating to the solar-thermal circuit, with heat-pump heating reserved for emergencies, protects winter battery autonomy and saves ≈ 40,800 TL versus a multi-split alternative.
- Against a continuous generator baseline, the system pays back in ~6 years and avoids ~2,770 kg CO_2/yr (~69 t over

25 years); LCOE is most sensitive to battery price and collector area.
- Winter heating, when both solar-thermal and PV supplies are lowest, and the 185 L boiler offers limited storage, is the binding constraint; evacuated-tube collectors and completion of the PVT retrofit are the most promising routes to a higher solar fraction and exergy efficiency.

Future work will validate the model against measured data from the installed prototype, complete the PVT retrofit and 35° re-mounting, and extend the EMS with predictive dispatch. The methodology is transferable to other seismically active, continental-climate regions where emergency housing and solar resources coincide.

Acknowledgements
This work was supported by the Scientific Research Projects (BAP) Coordination Office of OSTİM Technical University (Project No. BAP202522). The author thanks the Disaster and Emergency Management Authority of Türkiye (AFAD) for providing the container unit.

Ethical issue
The author is aware of and complies with best practices in publication ethics, specifically concerning authorship (avoidance of guest authorship), dual submission, manipulation of figures, competing interests, and compliance with policies on research ethics. The author adheres to publication requirements that the submitted work is original and has not been published elsewhere in any language.

Data availability statement
The manuscript contains all the data. However, more data will be available upon request from the corresponding author.

Conflict of interest
The author declares no potential conflict of interest.

References
[1] AFAD (Disaster and Emergency Management Authority). 2023 Kahramanmaraş (Pazarcık and Elbistan) Earthquakes Report. Ankara: AFAD; 2023. www.sbb.gov.tr/wp-content/uploads/2023/03/2023-Kahramanmaras-and-Hatay-Earthquakes-Report.pdf
[2] Republic of Türkiye, Presidency Directorate of Communications / AFAD. Integrated Disaster Management-Efforts in the Earthquake Zone (status report, February 2025). Ankara; 2025.
[3] International Energy Agency. Emissions Factors 2025 — Database Documentation. Paris: IEA; 2025. (Türkiye grid CO_2 factor ≈ 0.4–0.5 kg CO_2/kWh).
[4] Poredoš P, Tomc U, Petelin N, Vidrih B, Flisar U, Kitanovski A. Numerical and experimental investigation of the energy and exergy performance of solar thermal, photovoltaic and photovoltaic–thermal modules based on roll-bond heat exchangers. Energy Convers Manag. 2020;210:112674. https://doi.org/10.1016/j.enconman.2020.112674
[5] Çiftçi E, Khanlari A, Sözen A, Aytaç İ, Tuncer AD. Energy and exergy analysis of a photovoltaic thermal (PVT) system used in solar dryer: a numerical and experimental investigation. Renew Energy. 2021;180:410–423. https://doi.org/10.1016/j.renene.2021.08.081
[6] Hoarcă IC, Bizon N, Șorlei IS, Thounthong P. Sizing design for a hybrid renewable power system using HOMER and iHOGA simulators. Energies. 2023;16(4):1926. https://doi.org/10.3390/en16041926
[7] Mohamed MA, et al. Techno-economic and environmental analysis of a fully renewable hybrid energy system for sustainable power infrastructure. Sci Rep. 2025;15. https://doi.org/10.1038/s41598-025-96401-z
[8] Kallio S, Siroux M. Exergy and exergy-economic approach to evaluate hybrid renewable energy systems in buildings. Energies. 2023;16(3):1029. https://doi.org/10.3390/en16031029
[9] Petela R. Exergy of undiluted thermal radiation. Sol Energy. 2003;74(6):469–488. https://doi.org/10.1016/S0038-092X(03)00226-3
[10] Caliskan H. Energy, exergy, environmental, enviroeconomic, exergoenvironmental (EXEN) and exergoenviroeconomic (EXENEC) analyses of solar collectors. Renew Sustain Energy Rev. 2017;69:488–492. https://doi.org/10.1016/j.rser.2016.11.203
[11] Tashtoush B, Morosuk T, Chudasama J. Exergy and exergoeconomic analysis of a cogeneration hybrid solar organic Rankine cycle with ejector. Entropy. 2020;22(6):702. https://doi.org/10.3390/e22060702
[12] Tillmann P, Jäger K, Becker C. Minimising the levelised cost of electricity for bifacial solar panel arrays using Bayesian optimisation. Sustain Energy Fuels. 2020;4(1):254–264. https://doi.org/10.1039/C9SE00750D
[13] Preger Y, Barkholtz HM, Fresquez A, Campbell DL, Juba BW, Román-Kustas J, Ferreira SR, Chalamala B. Degradation of commercial lithium-ion cells as a function of chemistry and cycling conditions. J Electrochem Soc. 2020;167(12):120532. https://doi.org/10.1149/1945-7111/abae37
[14] Olmos J, Gandiaga I, Saez-de-Ibarra A, Larrea X, Nieva T, Aizpuru I. Modelling the cycling degradation of Li-ion batteries: chemistry influenced stress factors. J Energy Storage. 2021;40:102765. https://doi.org/10.1016/j.est.2021.102765
[15] Sayfutdinov T, Vorobev P. Optimal utilization strategy of the $LiFePO_4$ battery storage. Appl Energy. 2022;316:119080. https://doi.org/10.1016/j.apenergy.2022.119080
[16] Naumann M, Spingler FB, Jossen A. Analysis and modeling of cycle aging of a commercial $LiFePO_4$/graphite cell. J Power Sources. 2020;451:227666. https://doi.org/10.1016/j.jpowsour.2019.227666
[17] Zafra RG, Mayo JRM, Villareal PJM, De Padua VMN, Castillo MHT, Sundo MB, Madlangbayan MS. Structural and thermal performance assessment of shipping container as post-disaster housing in tropical climates. Civ Eng J. 2021;7(8):1437–1458. https://doi.org/10.28991/cej-2021-03091735
[18] Noaman DS, El-Ghafour SA. Holistic design of energy-efficient temporary houses: meeting ventilation, heating, cooling and lighting demands. J Build Eng.

2024;86:108534. https://doi.org/10.1016/j.jobe.2024.108534

[19] Tanyer AM, Tavukcuoglu A, Bekboliev M. Assessing the airtightness performance of container houses in relation to its effect on energy efficiency. Build Environ. 2018;134:59–73. https://doi.org/10.1016/j.buildenv.2018.02.026

[20] Tong Y, Yang H, Bao L, Guo B, Shi Y, Wang C. Analysis of thermal insulation thickness for a container house in the Yanqing zone of the Beijing 2022 Winter Games. Int J Environ Res Public Health. 2022;19(24):16417. https://doi.org/10.3390/ijerph192416417

[21] Mauro A, et al. Climate characterization and energy efficiency in container housing: implications for container house design in European locations. Energies. 2024;17(12):2926. https://doi.org/10.3390/en17122926